We are IntechOpen,
the world's leading publisher of
Open Access books
Built by scientists, for scientists

4,800
Open access books available

122,000
International authors and editors

135M
Downloads

Our authors are among the

154
Countries delivered to

TOP 1%
most cited scientists

12.2%
Contributors from top 500 universities

BOOK CITATION INDEX
CLARIVATE ANALYTICS
INDEXED

WEB OF SCIENCE™

Selection of our books indexed in the Book Citation Index
in Web of Science™ Core Collection (BKCI)

Interested in publishing with us?
Contact book.department@intechopen.com

Numbers displayed above are based on latest data collected.
For more information visit www.intechopen.com

p-type Phosphorus Doped ZnO Wires for Optoelectronic Applications

B. Q. Cao[2,1], M. Lorenz[1], G. Zimmermann[1], C. Czekalla[1], M. Brandt[1],
H. von Wenckstern[1], and M. Grundmann[1]
[1]Institut für Experimentelle Physik II, Universität Leipzig, Leipzig,
[2]School of Materials Science and Engineering, University of Jinan, Shandong,
[1]Germany
[2]China

1. Introduction

Semiconductor nanowires are especially attractive building blocks for assembling active and integrated nanosystems since the individual nanostructures can function as both device elements and interconnects. Among wide band gap II-VI semiconductors, ZnO seems to be one of the most promising materials for optoelectronic applications. This is due to its stable excitons, having a large binding energy of 60 meV [Ellmer et al., 2008, Jagadish & Pearton, 2006], which is important for applications of UV light-emitting devices and laser diodes with high efficiency. Therefore, growth of p-type conductive ZnO material is a prerequisite step since ZnO is intrinsically n-type [Look et al., 2001]. The growth of semiconductor nanowires with reproducible electronic properties, including the controlled incorporation of n-type and/or p-type dopants, has been realized in silicon, indium phosphide, and gallium nitride [Lieber & Wang, 2007]. In comparison with the semiconductors mentioned above, doping of ZnO seems more difficult not only for wires but films and bulk crystals due to the low dopant solubility and the self-compensation effect of intrinsic defects [Park et al., 2002]. It is also desired to more deeply understand the underlying doping physics [Zhang et al., 2001] for the achievement of a high-quality compound-semiconductor p-n junction.

Until now, there are only few reports on doped ZnO nanowires for p-type conductivity, possibly due to the obvious difficulties in both growth and optical/electrical characterization. Liu et al. [2003] prepared boron-doped ZnO nanowires and ZnO:B/ZnO nanowire junction arrays by a two-step vapor transport method in pores of anodic aluminum oxide membrane. A p-n junction-like rectifying behavior was observed. Lin et al. [2005] also reported a p-n rectification behavior of nitrogen doped ZnO (ZnO:N) nanowires/ZnO film homojunctions, where the ZnO:N nanowires were prepared by a post-growth NH_3 plasma treatment. Both reports did not contain any optical or electrical characterization of single (probably p-type) doped ZnO nanowires. Lee et al. [2004] prepared arsenic-doped ZnO nanowires by post annealed ZnO nanowires grown on GaAs substrate and observed arsenic induced acceptor bound exciton emission at 3.358 eV. Shan et al. [2007] reported the preparation of arsenic and phosphorus (co)doped ZnO nanowires also by an annealing method using ZnSe nanowires and GaAs/InP substrates as precursor and dopants, respectively. Recently, Xiang et al. [2007]

reported the p-type ZnO nanowire growth with chemical vapor deposition using phosphorus as dopants. The p-type conductivity of the doped wires was illustrated with gate-voltage dependent conductance measurements of single ZnO:P nanowires with field effect transistor (FET) configuration. However, p-type conductivity was not stable and converted to n-type three months later. Similarly, Yuan et al. [2008] reported the growth by chemical vapor deposition (CVD) of nitrogen doped ZnO wires which showed p-type FET characteristics. Lu et al. [2009] reported the growth of p-type ZnO nanowires also with CVD using Zn_3P_2 as dopant. Moreover, energy conversion using the p-type ZnO NWs has also been demonstrated and the p-type ZnO NWs produce positive output voltage pulses when scanned by a conductive atomic force microscope (AFM) in contact mode while the n-type nanowires produced a negative voltage signal. Consequently, it seems that doped p-type ZnO wires come into reality. But, the doping induced optical fingerprints were not clearly identified and p-n junctions built from p-type ZnO nanowires are still not available.

In this Chapter, after the brief review of the research progress on p-type ZnO wires, some important results obtained in our group on p-type ZnO nanowires and microwires are summarized. In the second section, the high-pressure pulsed laser deposition (PLD) and carbothermal evaporation growth methods for doped wire growth will be described. Optical and electrical characterizations of the doped wires will be discussed in detail in the third section. This Chapter ends with a brief summary, which also includes our personal remarks on future research of p-type ZnO wires.
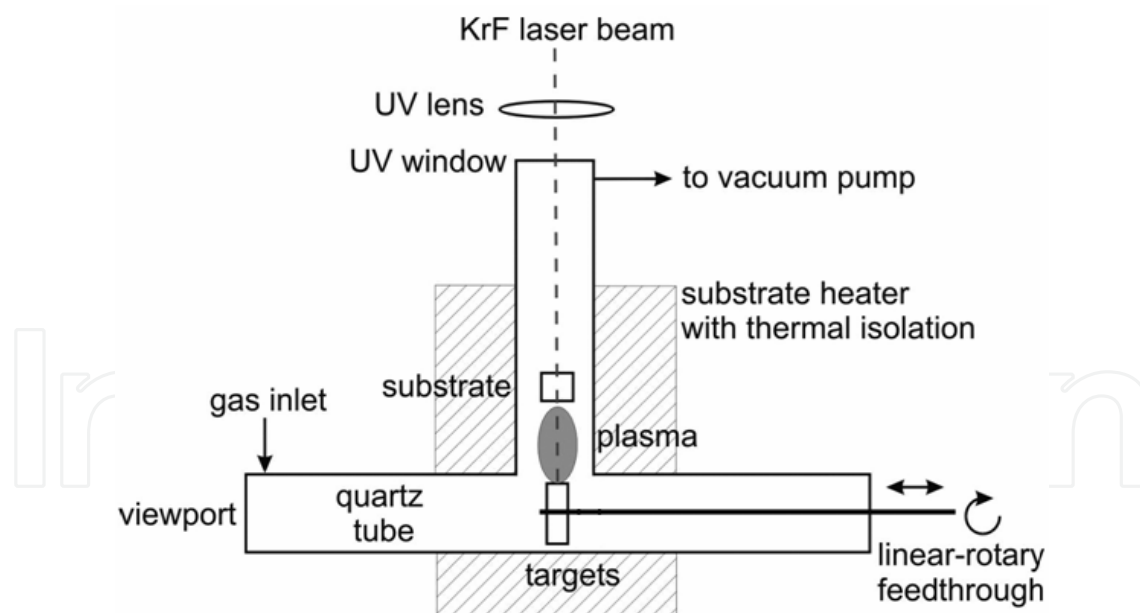
2. Growth of phosphorus doped ZnO wires

Fig. 1. Schematic illustration of the high-pressure PLD chamber for pure and doped ZnO nanowire growth with a T-shaped quartz tube. From Ref. [Lorenz et al., 2005].

Two methods, high-pressure pulsed laser deposition and carbothermal evaporation, were applied to grow phosphorus doped ZnO wires with diameter varied from 100 nm to 10μm. PLD is a well established growth method for thin films by condensation of laser plasma ablated from a target, excited by the high-energy laser pulses far from equilibrium [Willmott

& Huber, 2000]. Figure 1 shows the scheme of the high-pressure PLD chamber specially designed for ZnO nanostructures using a T-shaped quartz tube with an outer diameter of 30 mm in the Leipzig semiconductor physics group [Lorenz et al., 2005]. A KrF excimer laser beam enters along the center of the tube and is focused on the cylindrical surface of the selected targets. The laser energy density on the target is about 2 J/cm², which is similar to conventional PLD film growth conditions. An encapsulated heater with an arrangement of KANTHAL wire in ceramic tubes and FIBROTHAL isolation material is built around the T-shape quartz tube. The growth temperature is usually chosen between 500 and 950 ˚C as measured by a thermocouple. Argon flow of 0.05 to 0.2 l/min was usually selected as carrier gas and the growth pressure ranged between 25 and 200 mbar. The a- or c-plane sapphire substrates (size 1×1 cm²) were arranged of-axis, i.e. parallel to the expanding plasma plume. PLD generally facilitates stoichiometric transfer of the chemical composition of a multielement source target into the grown samples [Chrisey & Hubler, 1994]. Therefore, if the ablated target is doped, the corresponding samples are expected to have the similar composition to the targets. For phosphorus doping of ZnO nanowires, phosphorus pentoxide (P_2O_5) was select as dopants for acceptors. Figure 2 shows a scanning electron microscopy (SEM) image of ZnO wires using doped ZnO targets with different P_2O_5 concentration. Figure 3 shows typical energy dispersive x-ray spectroscopy (EDX) results detected from a single doped nanowire. The phosphorus signal is clearly observed. The
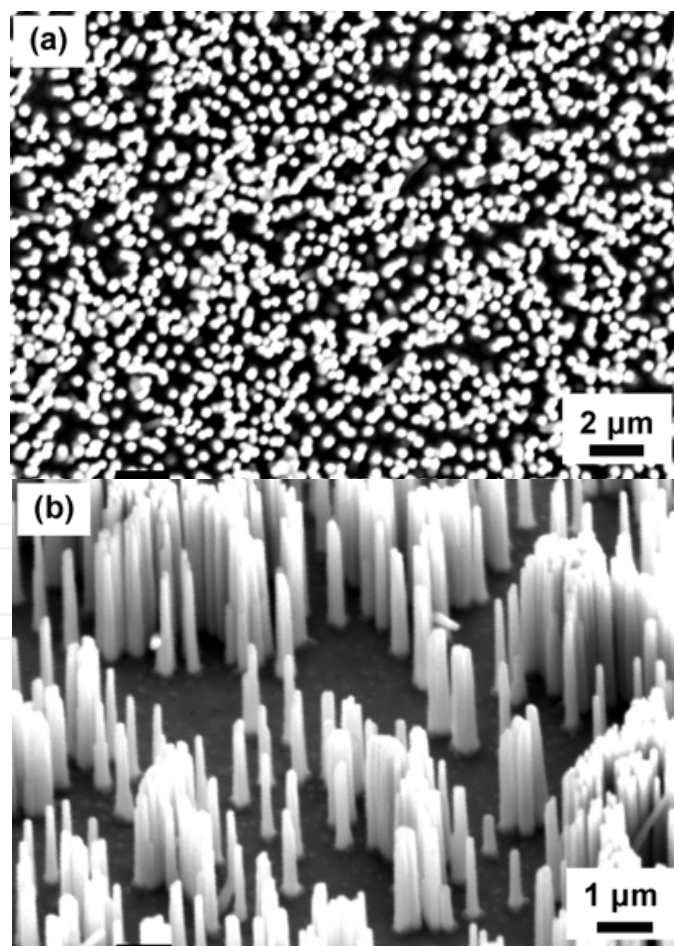

Fig. 2. SEM images of ZnO:P wire grown with PLD using (a) 1 wt% P_2O_5 and (b) 2 wt% P_2O_5 doped ZnO targets at 100 Torr and 900 ˚C.

weight percentage of phosphorous in the nanowire is about 1 wt%, which is smaller than the phosphorus concentration (1.7 wt%) in the target. This is probably caused by the different vapor pressures of zinc and phosphorus related species in the laser ablated plume and different sticking coefficients [Ohtomo et al., 1998].
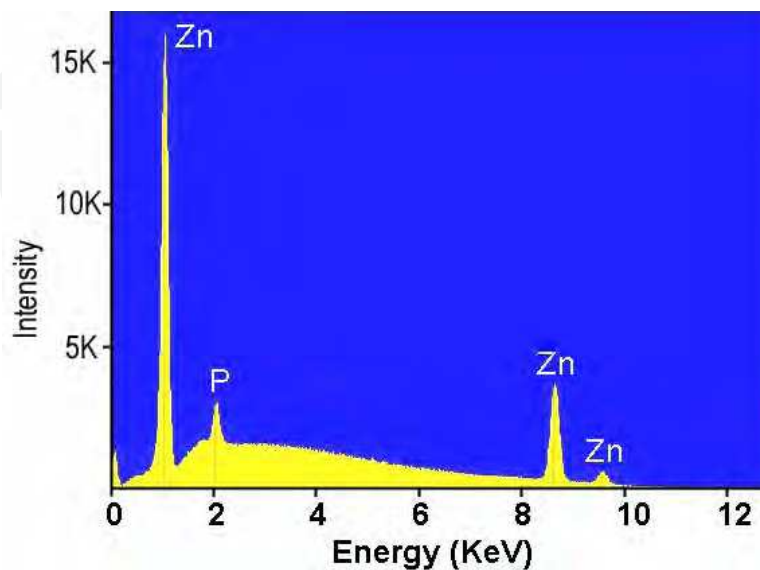

Fig. 3. Energy dispersive x-ray spectrum of a single doped ZnO:P wire with obvious phosphorus signal, excited by electron beam in a SEM.
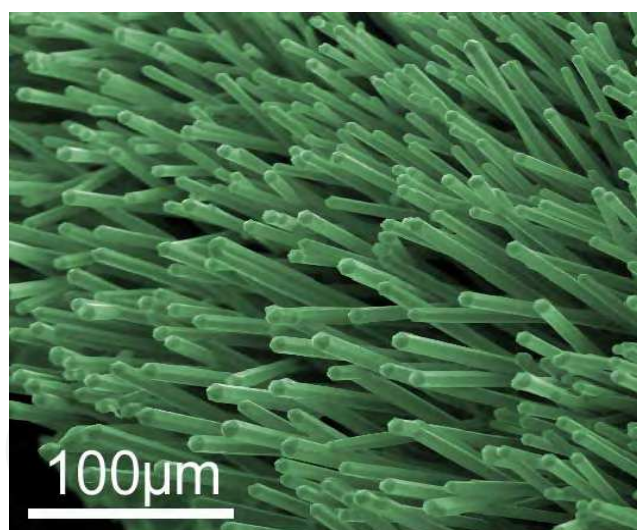

Fig. 4. A typical SEM image of doped ZnO microwires grown directly on pressed source material target. From Ref. [Cao et al., 2008].

In our group, vapor phase transport and deposition process was also employed for the growth of ZnO nanowires and microwires, as proposed by Huang and Yao [Huang et al., 2001; Yao et al., 2002]. This method, also called carbothermal evaporation, is widely used for growth of nanowires, and it has relations to other methods, such as chemical vapor deposition (CVD), metal-organic chemical vapor deposition (MOCVD), physical vapor deposition (PVD). Carbothermal evaporation has been conventionally used to synthesize one-dimensional and other complex oxide nanostructures, including ZnO as reviewed

recently by Wang et al. [2009]. Here, the standard process was developed to synthesize doped ZnO microwires by direct thermal evaporation of a pressed ZnO/graphite (mass ratio 1:1) target doped with P_2O_5 (15 wt%) at ambient pressure. The growth temperature was as high as 1100 °C and the microwires grew directly on the pressed target. Figure 4 shows a typical SEM image of doped ZnO microwires produced by this method. Such microwires are easily visible with optical microscopy and, therefore, are more convenient for device fabrications.

3. Optical and electrical properties of ZnO:P wires
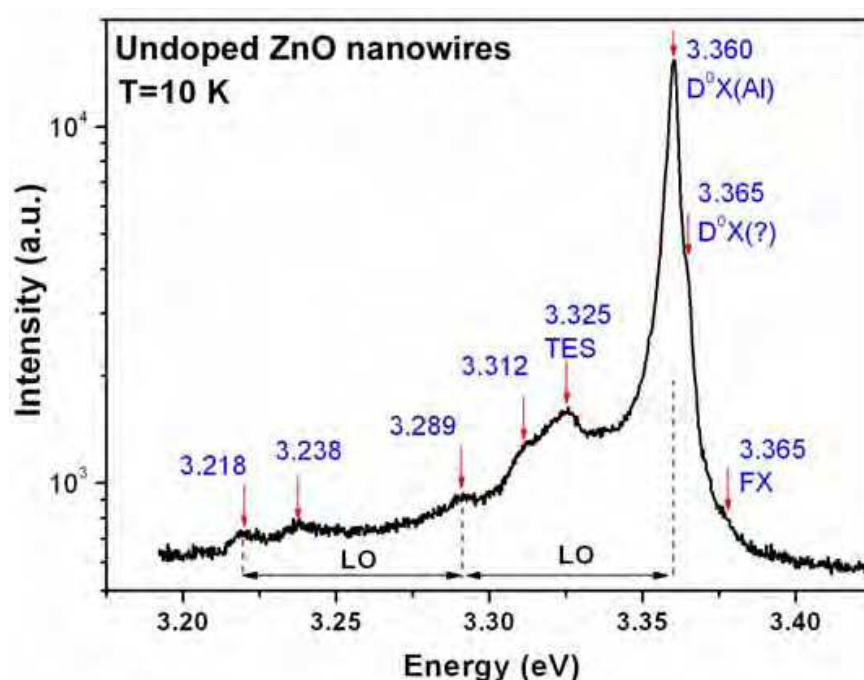
3.1 Optical properties of ZnO:P wires

Fig. 5. CL spectrum of undoped ZnO nanowires measured at a temperature of 10 K.

To study the doping effect on the physical properties of ZnO nanowires and also identify the conductivity type of the doped nanowires, optical properties were first investigated by cathodoluminescence (CL) spectroscopy. More detailed description of the CL measurement system can be found in Ref. [Nobis et al., 2004].

A low temperature CL spectrum at *T*=10 K of undoped ZnO nanowires grown with PLD using pure ZnO target is shown in Figure 5. It is dominated by an emission peak at 3.360 eV (I_6) originating from the aluminum-related neutral donor-bound excitons (D^0, X) [Meyer et al., 2004]. On the high energy side of this peak, the minor peaks at 3.365 and 3.377 eV are the I_{3a} donor-bound exciton and the free-exciton (FX) recombination, respectively. The peak at 3.325 eV is due to two-electron satellite (TES) emission. The weak peaks in the lower energy range from 3.20 eV to 3.33 eV are the optical phonon replicas of the D^0X.

Figure 6(a) depicts the CL spectra of a single ZnO:P nanowire measured at three points as indicated, which show similar spectroscopic features. The spectra are clearly different from that of undoped ZnO nanowires. Three groups of new emission peaks at 3.356, 3.314, 3.234
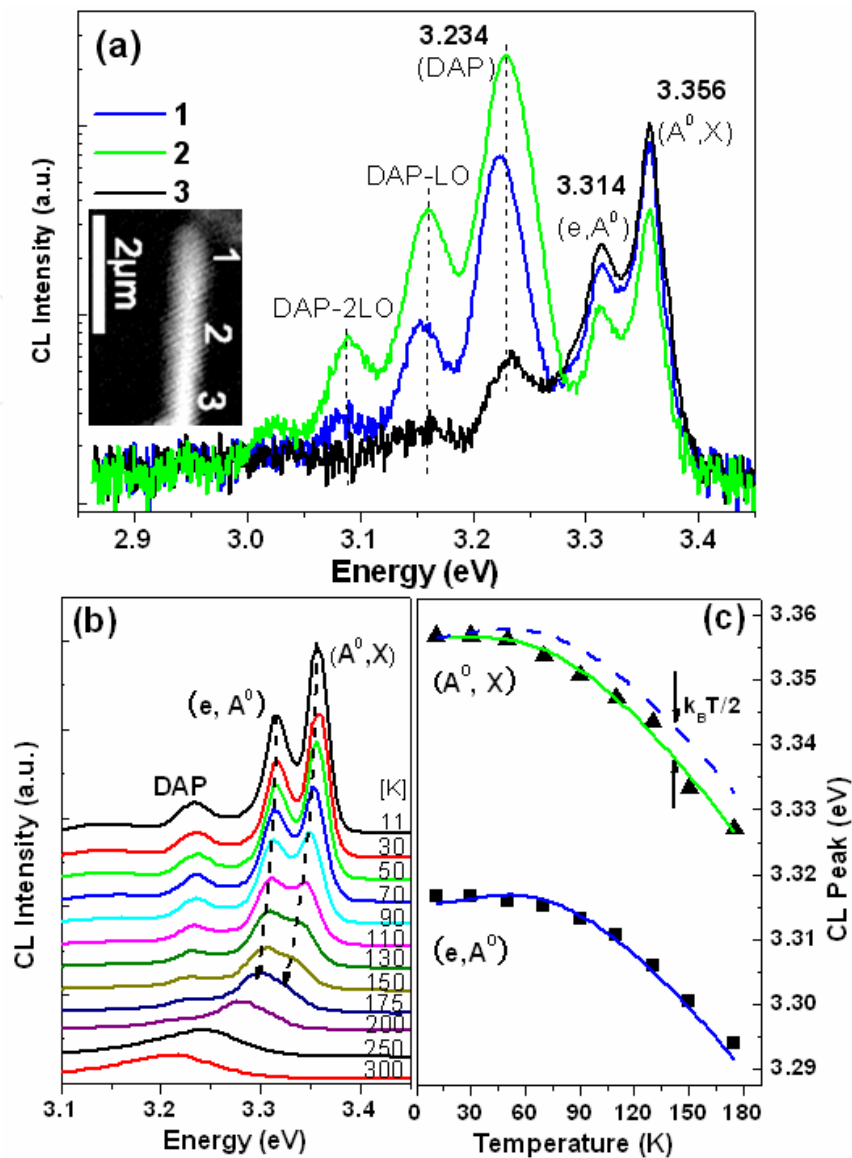
Fig. 6. (a) CL spectra at temperature of 10 K of a single ZnO:P nanowires measured at three parts, as indicated in the inset. (b) Temperature-dependent CL spectra of ZnO:P nanowires. (c) CL peak energies versus temperatures taken from (b). Solid symbols (■ and ▲) are experimental data and solid lines are fitted with equations [1] and [2], respectively. The dashed line is shifted to demonstrate the slope of the (e, A^0) fitted line (blue) near the (A^0, X) data points. From Ref. [Cao et al., 2007].

eV and their phonon replica were detected. It indicates that these emission peaks are due to the intentional phosphorous doping. The peak at 3.356 eV can be ascribed to the phosphorus-related neutral acceptor-bound exciton (A^0, X) emission [Hwang et al., 2005, Vaithianathan et al., 2005]. As for the peak at 3.314 eV, it is a prominent optical characteristic of most p-type ZnO material doped with group V elements. But, its origin is still a matter of debate [Look, 2005]. The origin of the dominant peak at 3.234 eV is also controversial. But, it shows strong longitudinal phonon replica that means that it comes from acceptor-related recombination process due to the phosphorus doping of ZnO. Because, for donor-related lines, only weekly coupling phonon lines can be observed, as shown in Figure 5. Therefore,

the peaks at 3.314 and 3.234 eV could be tentatively ascribed respectively to free electron-to-acceptor (e, A^0) emission and donor-to-acceptor pair (DAP) emission in agreement with the discussion of nitrogen doped ZnO [Xiong, 2005].

Temperature-dependent luminescence behavior usually can prove the origin of the near-band-gap emissions of semiconductors. Figure 6(b) shows the temperature-dependent CL spectra of ZnO:P nanowires. The peak of (A^0, X) shows a continuous redshift due to the bandgap shrinkage with increasing temperature, which can be well fitted by the Bose-Einstein model [O'Donnell & Chen, 1991],

$$E_{A^0,X}(T) = E_{A^0,X}(0) - 2\alpha_B \Theta_B [\coth\left(\frac{\Theta_B}{2T}\right) - 1] ,$$ (1)

with $E_{A^0,X}(0)$=3.356 eV, a_B=1.2($\pm$0.2)*10^{-4} eV/K, and Θ_B=306($\pm$45) K. Its intensity decreases gradually, and eventually vanishes above 175 K due to the ionization of excitons from the acceptor. In this process, no emission of free exciton (FX) can be observed due to the dissociation of free excitons into free electrons and holes caused by the potential fluctuations of the band edges. It suggests that a high concentration of phosphorous dopants has been incorporated. The DAP peak intensity also decreases gradually with increasing temperature and finally disappears above 200 K. This temperature-dependent behavior is typical for the thermal ionization of shallow donors via the pathway of (D^0, A^0) $\rightarrow D^+ + A^0 + e$. The ionized free electrons in the conduction band prefer to recombine with acceptors. As a result, the spectra are dominated by (e, A^0) at temperatures of 130-175 K. Figure 6 (c) also depicts the peak energy of (e, A^0) can be fitted with

$$E_{e,A0}(T) = E_g(T) - E_A + \frac{1}{2}k_B T ,$$ (2)

where $E_{e,A^0}(T)$, $E_g(T)$, and E_A are the peak position of (e, A^0), band gap, and binding energy of the acceptor, respectively. The fitting coefficients α_B and Θ_B were taken from the fitted values of (A^0, X) with Eq. (1). The fitted E_A of phosphorus acceptor is 122 ($\pm$1) meV. It is noted that the temperature dependence of (A^0, X) differs from that of (e, A^0) by $k_B T/2$, which is also the character of the free electron-to-acceptor transition [Ye et al., 2007]. In summary, the temperature-dependent CL results provide additional evidence by optical fingerprints of the phosphorus acceptor recombination in ZnO.

3.2 Electrical properties of ZnO:P wires

Homogeneous doped semiconductor nanowires represent key building blocks for a variety of electronic devices. After confirming the successful incorporation of phosphorus acceptors into the ZnO nanowires, the next step to identify the conductivity of the doped nanowires would be electrical measurements by device fabrication, which are always highly desirable. As direct Hall measurements on nanowires are difficult since the necessary two-dimensional configuration of the Hall contacts is hard to achieve, other practicable methods to obtain the conducting type of nanowires are adopted. In this section, p-n junction and field effect transistor (FET) structures were proposed and built with ZnO:P wires for electrical studies.

3.2.1 ZnO:P nanowires / ZnO:Ga film p-n homojunction

p-n junctions are of great importance both in modern electronic application and in understanding other semiconductor devices. A typical proposed two-terminal junction composed of doped nanowires and n-type ZnO:Ga film was shown in Figure 7(a). It was completely grown with PLD.
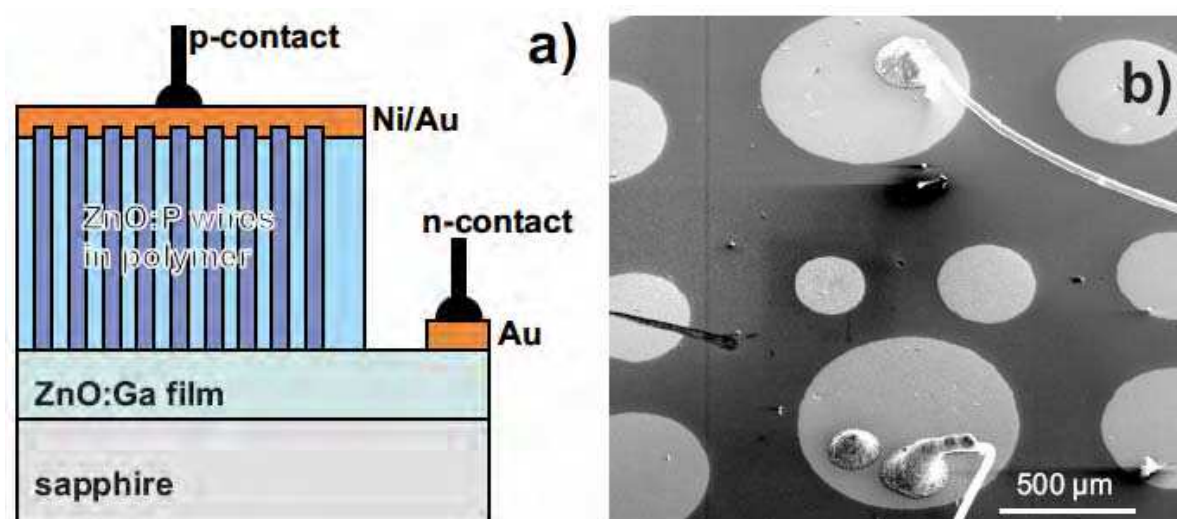

Fig. 7. (a) Scheme of the ZnO:P/ZnO:Ga p-n junctions including one p- and one n-contact. (b) A top view on the Ni–Au contact pads on top of the embedded ZnO:P nanowire array. The connection to the bond wires is made with silver glue. From Ref. [Lorenz et al., 2009].

Gallium-doped, n-type conducting ZnO thin films were grown with conventional low-pressure PLD using a ZnO:Ga (5 wt%) target. After deposition of the gold contact strip, these ZnO:Ga film templates were transferred into the high-pressure PLD chamber for growth of the ZnO:P nanowire arrays. The growth conditions were similar to that described in Section 2. After the nanowire growth, the samples were a spin-coated with polystyrene and then exposed to RF plasma at air pressure of 3×10^{-2} mbar to free the nanowires' tips from the polystyrene. Finally, Ni/Au top contacts were deposited with a mask on the top of the polystyrene and contacted with gold wire using conductive silver glue. Figure 7(b) shows a SEM image the top-view of the junction device.

Figure 8(a) shows the I-V curves measured from p_1-n and p_2-n, which are two parallel junction structures. The rectifying I-V behavior of the phosphorus doped wires on n-type ZnO film can be reproducibly observed from ten samples with over 50 p-n junctions. Moreover, the reverse parts of the I-V curves measured from p_1-n, and p_2-n agree reasonably well with the I-V curve of p_1-n-p_2, which is composed of two p-n junction diodes both under reverse bias. This is a strong indication for the p-type conductivity of the doped ZnO:P nanowires. The typical voltage for I=100 µA of the p-n junctions is up to 3.2 V and the forward to reverse current ratio is about 100 at ±3.5 V. The series resistance R_s of the p-n junction is about 23 kΩ. The low-voltage forward parts of the I-V curves were fitted with the equation $I=I_s\{\exp[e(V-R_sI)/nk_BT]-1\}$, i.e., the I-V characteristics of a real diode with negligible shunt resistance, as shown in Figure 8(b). The ideality factor n of the particular junction in Figure 8 was about 7.
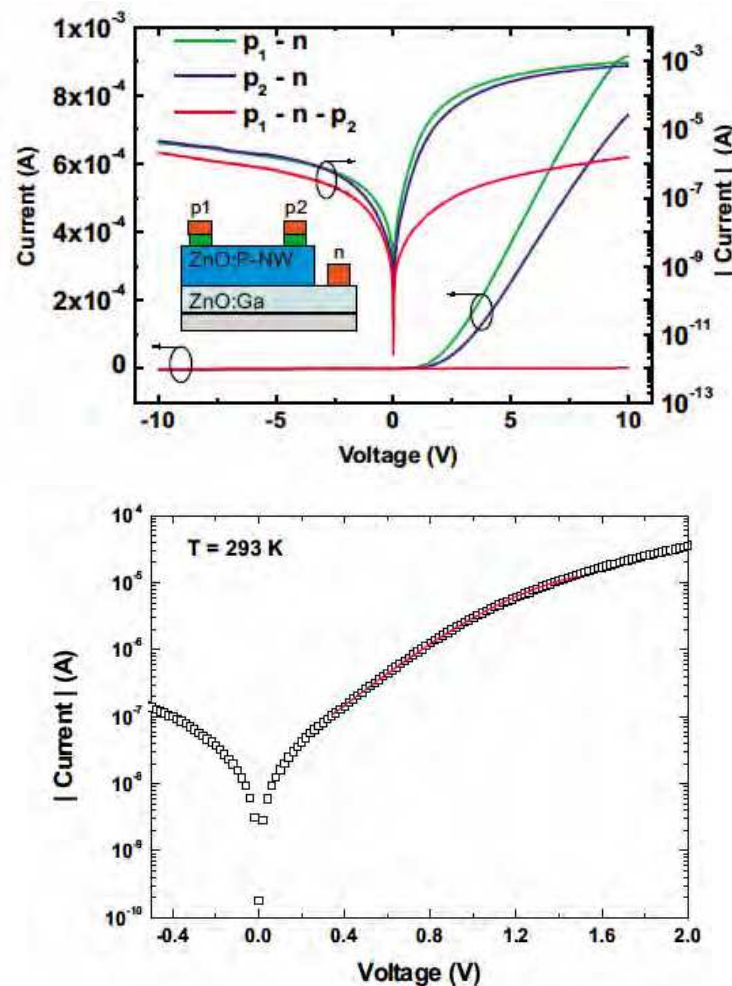
Fig. 8. (a) Rectifying I-V curves of two typical ZnO p-n junctions on the same substrate, denoted p_1-n and p_2-n, plotted in both linear and logarithmic current scale. The I-V curves of these two p-contacts is also shown, which corresponds to the p_1-n-p_2 configuration of two opposite p-n diodes. (b) I-V curve fitted with the equation, I =I_s\{exp[e(V-R_sI)/nk_BT]−1\} (red curve), to a typical p-n junction (open squares). The fit results are as follows: I_s=15.8 nA; R_s=23.0 kΩ; n=7.03. From Ref. [Lorenz et al., 2009].

3.2.2 p-type ZnO:P microwire FET

Another prototypical semiconductor device with broad applications is the nanowire FET. Nanowires configured as FETs have shown to operate at ultralow power below microwatts with enhanced operation speed. For example, studies of nanowire FETs fabricated from boron and phosphorus-doped Si nanowires have shown that the devices can exhibit performance comparable to the best reported value for planar devices made from the same materials [Cui et al., 2003]. Studies have also demonstrated the high electron mobility of epitaxial InAs nanowire FETs with a wrap-around cylindrical gate structure surrounding a nanowire [Thelander et al., 2008]. Moreover, the change in conductance of semiconductor wires as a function of gate voltage can be used to determine the conductive type of a given wire since the conductance will vary oppositely for increasing positive and negative gate voltages [Cui et al., 2003]. Therefore, the FET characteristics analyses were also used to study the doping effect of semiconductor nanowires.
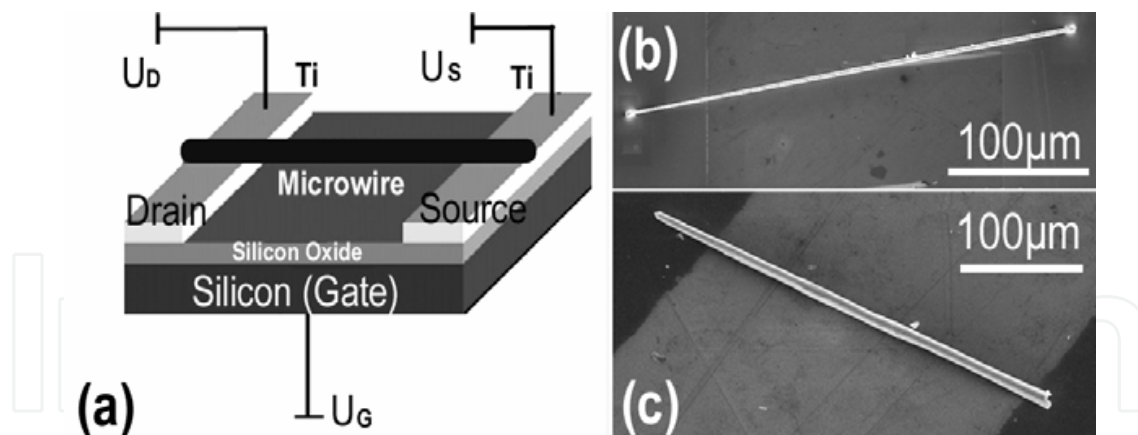
Fig. 9. (a) Schematic illustration of the back-gate FET configured with a microwire as conductive channel. (b) SEM image of a undoped ZnO microwire fixed on titanium electrodes with IBID. (c) SEM image of phosphorus doped ZnO microwire directly connecting with two titanium contacts.

Figure 9(a) schematically shows the FET structure assembled with a microwire. Silicon substrates (65 mΩcm) covered by a SiO_2 layer with thickness of 190 nm served as the global back-gate and dielectric gate oxide, respectively. Titanium strip contacts were then defined on such silicon substrates with photolithography. Then the microwires were transferred onto the predefined silicon substrate and laterally moved to connect them with titanium stripes, which formed the source and drain contacts. Figure 9(b) shows the SEM image of an undoped ZnO microwire FET, where the source and drain contact characteristics were further improved with tungsten contact pads deposited with ion-beam induced deposition (IBID). In this way, the contacts between ZnO wires and titanium strips are ohmic, as demonstrated in Figure 10(a) with the linear current-voltage dependence in a wide voltage range from -30 V to +30 V. The dependence of source-drain current (I_{SD}) through the ZnO wire on source-drain voltage (U_{SD}) was measured at various gate voltages, as shown in Figure 10(b). The I_{SD} increases with increasing U_{SD} and the slopes of the I_{SD} versus U_{SD} curves are dependent on the gate voltage (U_G). Figure 10(c) shows the corresponding transfer characteristics ($I_{SD} - U_G$) at a constant U_{SD} of 2 V. In general, the source-drain current increases with increasing gate voltage. This positive slope of the I_{SD} vs. U_G curve indicates that the undoped ZnO wire is n-type conducting. It has to be noted that usually the ZnO wire channel could not be fully depleted with such a back-gate configuration. A possible reason is the finite air gap between the gate oxide and the ZnO wire [Keem et al., 2007].

Because gallium is a donor in ZnO, the source and drain contacts of the doped ZnO:P microwire FETs were formed by connecting the ZnO:P wire directly to two separated titanium electrodes, as seen in Figure 9(c), without further FIB support [Weissenberger et al., 2007]. Therefore, the electrical characteristics of the ZnO:P wire-FETs are sensitively dependent on the particular contacts between the wire and electrodes. Figure 11 shows two groups of typical current-voltage ($I_{SD} - U_{SD}$) curves of ZnO:P wire-FETs under different back-gate voltages. All curves are slightly nonlinear, which indicates that the contacts between wire and titanium electrodes are not ideally ohmic. However, in both graphs of Figure 11 the $I_{SD} - U_{SD}$ curves show an inverse arrangement concerning the gate voltage
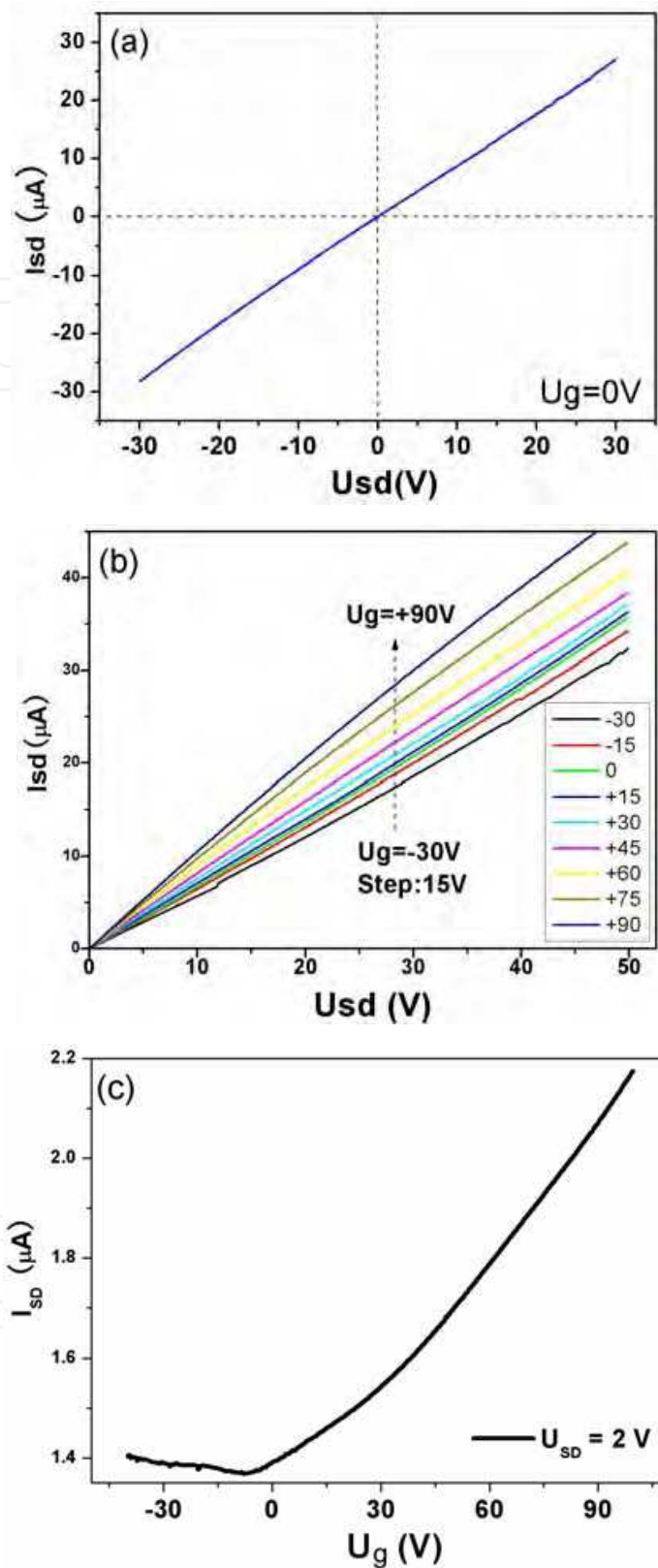
Fig. 10. (a) I_{SD} vs U_{SD} curve at U_G=0 V indicating good ohmic contacts between ZnO wires and titanium strips; (b) Output characteristics I_{SD} vs U_{SD} and (c) transfer characteristics I_{SD} vs U_g of the nominally undoped, n-type ZnO microwire FET. From Ref. [Cao et al., 2008].
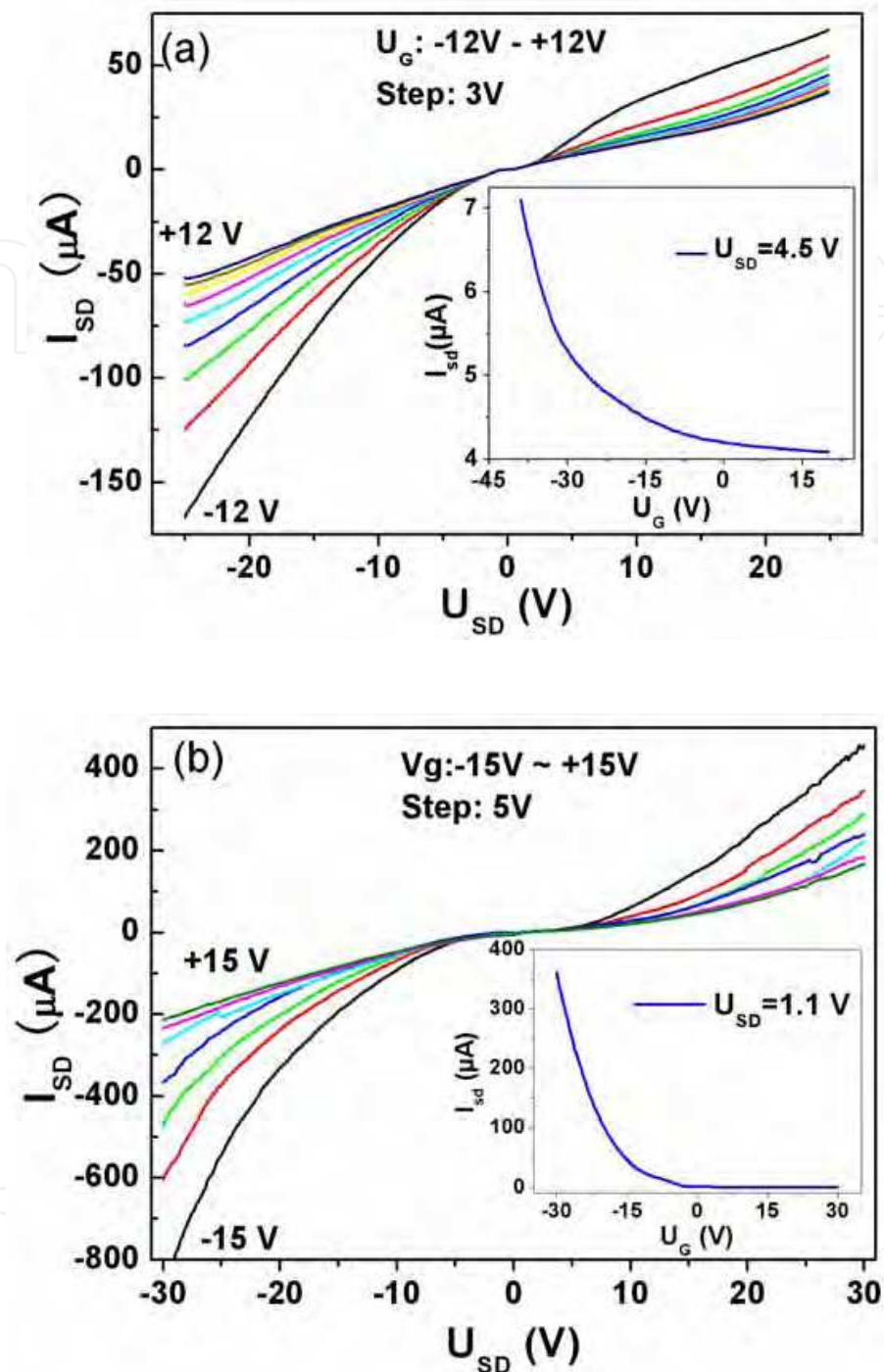
Fig. 11. Output characteristics (I_{SD} vs U_{SD}) and transfer characteristics (I_{SD} vs U_G, inset) of two different ZnO:P wire-FETs, indicating p-type conductivity of the doped ZnO microwires. From Ref. [Cao et al., 2008].

compared to that of the undoped n-type wire FET in Figure 10(b). This is further demonstrated by the insets of Figure 11, where the corresponding transfer characteristics of the ZnO:P wire FETs are shown. The source-drain current decreases with increasing gate

voltage. This negative I_{SD}-U_G slope is opposite to that of the undoped n-type ZnO-FET. It indicates unambiguously that the conductivity of the phosphorus doped ZnO wires is p-type. In most cases, such ZnO:P wire-FETs could not be fully depleted as shown in Figure 11(a). However, Figure 11(b) is an example of a fully depleted ZnO:P microwire channel.

At last, the time stability of the p-type conductivity of such ZnO:P wires were investigated by repeated FET and p-n junction measurements. p-type conducting FET characteristics built with microwires grown by carbothermal evaporation were reproducibly observed within six months since their growth. No obvious change of the FET characteristics was found. Thus the time stability of p-conductivity of the ZnO:P microwires is at least six months. As for the p-n junctions built with ZnO:P doped nanowires grown by PLD after one year, in total about 20 junction samples, about ten still showed the typical rectifying diode behavior as shown in Figure 8. Therefore, we can state a corresponding time stability of the ZnO junctions. Moreover, electroluminescence experiments with pulsed current excitation (6V/8mA peak current with 1 kHz and 10% duty cycle) on selected junctions showed a very weak, diffuse blue-green light emission. This light emission was visible to the naked eye in complete darkness.

4. Summary

In summary, we have reviewed the latest progress in the growth and optical/electrical characterizations of p-type doped ZnO wires, especially the work performed in the Leipzig group. Two growth methods, high-pressure PLD and carbothermal evaporation, have been adopted to grow phosphorus doped ZnO wires. Detailed optical and electrical characterizations of such doped wires indicated their p-type conductivity with one-year stability. In our opinion, more work is still needed to make further progress on this topic. First, the quality and stability of the p-type ZnO wires need to be further improved. This will require even better control the background n-type conductivity, development of new growth methods and search for new acceptor dopants. Second, high-quality p-n junctions built with single p-type ZnO nanowires showing good breakdown characteristics need to be demonstrated. Third, electrically pumped ZnO nanowire LED and laser diode showing strong band-edge emission are highly expected. Once these milestones are achieved, it would be the beginning of the ZnO applications for solid state lighting.

5. Acknowledgements

6. References

Cao B. Q.; Lorenz M.; Rahm A.; von Wenckstern H.; Czekalla C.; Lenzner J.; Benndorf G. & Grundmann M. (2007). Phosphorus acceptor doped ZnO nanowires prepared by pulsed-laser deposition, *Nanotechnology,* 18: 455707 (5 pages)

Cao B. Q.; Lorenz M.; Brandt M.; von Wenckstern H.; Lenzner J.; Biehne G. & Grundmann M. (2008) P-type conducting ZnO:P microwires prepared by direct carbothermal growth, *phys. stat. sol. (RRL)* 2(1): 37-39

Cao B. Q.; Lorenz M.; Brandt, von Wenckstern H.; Lenzner J.; Biehne G. & Grundmann M. (2008). p-type conducting ZnO:P microwires prepared by direct carbothermal growth, *phys. stat. sol. (RRL),* 2(1): 37-39.

Chrisey D. B. & Hubler G. K. (1994). *Pulsed laser deposition of thin films*, Wiley, ISBN: 978-0-471-59218-1, New York

Cui Y.; Zhong Z. H.; Wang D. L.; Wang W. U. & Lieber C. M. (2003). High performance silicon nanowire field effect transistors, *Nano Lett.* 3(2). 149-152.

Cui Y.; Duan X. F.; Hu J. T. & Lieber C. M. (2003). Doping and electrical transport in silicon nanowires, *J. Phys. Chem. B* 104(22). 5213-5216.

Ellmer K.; Klein A. & Rech B. (2008). *Transparent Conductive Zinc Oxide*, Springer, ISBN: 978-3-540-73611-0, Berlin, Heidelberg and New York

Huang M. H.; Wu Y. Y.; Feick H.; Tran N.; Weber E. & Yang P. D. (2001). Catalytic growth of zinc oxide nanowires by vapor transport, *Adv. Mater.* 13(2): 113-116

Hwang D. K.; Kim H. S.; Lim J. H.; Oh J.Y.; Yang J.H.; Park S. J.; Kim K. K.; Look D. C. & Park Y. S. (2005). Study of the photoluminescence of phosphorus-doped p-type ZnO thin films grown by radio-frequency magnetron sputtering, *Appl. Phys. Lett.* 86: 151917 (3 pages)

Jagadish C. & Pearton S. (2006). *Zinc Oxide Bulk, Thin films and Nanostructures: Processing, Properties and Applications,* Elsevier, ISBN: 978-0-08-044722-3, Amsterdam

Keem K. Y.; Kang J. M.; Yoon C. J.; Yeom D. H.; Jeong D. Y.; Moon B. M. & Kim S. S. (2007), A fabrication technique for top-gated ZnO nanowire field effect transistors by a photolithography process, *Microelectr. Eng.* 84: 1622-1626.

Lee W.; Jeong M. C. & Myoung J. M. (2004). Optical characteristics of arsenic-doped ZnO nanowires, *Appl. Phys. Lett.* 85(25): 6167 (3pages)

Lieber C. M & Wang Z. L. (2007). Functional Nanowires, *MRS Bulletin,* 32(Feb.): 99-108

Lin C. C.; Chen H. P. & Chen S. Y. (2005). Synthesis and optoelectrical properites of arrayed p-type ZnO nanorods grown on ZnO film/Si wafer in aqueous solutions, *Chem. Phys. Lett.* 404: 30-34

Liu C. H.; Yiu W. C.; Au. F. C. K. ; Ding J. X.; Lee C. S. & Lee S. T. (2003), Electrical properties of zinc oxide nanowires and intramolecular p-n junctions, *Appl. Phys. Lett.* 83(15): 3168 (3 pages)

Look D. C.; Claflin B.; Alivov Ya. I. & Park S. J. (2001). The future of ZnO light emitters, *phys. stat. sol. (a),* 201(10): 2203-2212

Look D. C. (2005), Electrical and optical properties of p-type ZnO, *Semicond. Sci. Technol.* 20: S55-S61

Lorenz M.; Kaidashev E. M.; Rahm A.; Nobis Th.; Lenzner J.; Wagner G.; Spemann D.; Hochmuth H. & Grundmann M. (2005). $Mg_xZn_{1-x}O$ (0≤x<0.2) nanowire arrays on sapphire grown by high-pressure pulsed-laser deposition, *Appl. Phys. Lett.* 86: 143113 (3 pages)

Lorenz M.; Cao B. Q.; Zimmermann G.; Biehne G.; Czekalla C.; Frenzel H.; Brandt M.; von Wenckstern H. & Grundmann M. (2009), Stable p-type ZnO:P nanowire/n-type

ZnO:Ga film junctions, reproducibly grown by two-step pulsed laser deposition, *J. Vac. Sci. Technol. B*. 27(3): 1693-1697.

Lu M. P.; Song J. H.; Lu M. Y. ; Chen M. T. ; Gao Y. F. ; Chen L. J. & Wang Z. L. (2009). Piezoelectric nanogenerator using p-type ZnO nanowire arrays, *Nano Lett.* 9(3): 1223-1227

Meyer B. K.; Alves H.; Hofmann D. M.; Kriegseis W.; Forster D.; Bertram F.; Christen J.; Hoffmann A.; Straßburg M.; Dworzak M.; Haboeck U. & Rodina A. V. (2004), Bound excitons and donor-acceptor pair recombinations in ZnO, *phys. stat. sol. (b)* 241(2): 231-260

Nobis T.; Kaidashev E. M.; Rahm A.; Lorenz M.; Lenzner J. & Grundmann M. (2004). Spatially inhomogenous impurity distribution in ZnO micropillars, *Nano Lett.* 4(5): 797-800.

O'Donnell K. P. & Chen X. (1991). Temperature dependence of semiconductor band gaps, *Appl. Phys. Lett.* 58: 2924 (3 pages)

Ohtomo A, Kawasaki M, Koida T, Masubuchi K, Koinuma H, Sakurai Y, Yoshida Y, Yasuda T and Segawa Y (1998). $Mg_xZn_{1-x}O$ as a II–VI widegap semiconductor alloy, *Appl.Phys. Lett.* 72: 2466 (3 pages)

Park C. H., Zhang S. B. & Wei S. H. (2002). Origin of p-type doping difficulty in ZnO: The impurity perspective, *Phys. Rev. B*. 66: 073202 (3 pages)

Shan C. X.; Liu Z.; Wong C. C. & Hark S. K. (2007). Doped ZnO nanowires obtained by thermal annealing, *J. Nanosci. Nanotech.* 7: 700-703

Thelander C.; Fröberg L. E.; Rehnstedt C.; Samuelson L. & Wernersson L. (2008). Vertical enhancement-mode InAs nanowire field-effect transistor with 50-nm wrap gate, *IEEE Electron Device Lett.* 29(3). 206-208.

Vaithianathan V.; Lee B. T. and Kim S. S. (2005). Pulsed-laser-deposited p-type ZnO films with phosphorus doping, *J. Appl. Phys.* 98: 043519 (4 pages)

Wang Z. L. (2009). ZnO nanowire and nanobelt platform for nanotechnology, *Mater. Sci. Eng. R.* 64: 33-71.

Weissenberger D.; Mürrschnabel M.; Gerthsen D.; Pérez-Willard F.; Reiser A.; Prinz G. M.; Feneberg M.; Thonke K. & Sauer R. (2007). Conductivity of single ZnO nanorods after Ga implantation in a focused-ion-beam system, *Appl. Phys. Lett.* 91: 132110 (3 pages)

Willmott P. R. & Huber J. R. (2000). Pulsed laser vaporization and deposition, *Rev. Mod. Phys.* 72(1): 315-328

Xiang B.; Wang P. W.; Zhang X. Z.; Dayeh S. A.; Aplin D. P. R.; Soci C.; Yu D. P. & Wang D. L. (2007). Rational synthesis of p-type Zinc oxide nanowire arrays using simple chemical vapor deposition, *Nano Lett.* 7(2): 323-328

Xiong G.; Ucer K. B.; Williams R. T.; Lee J.; Bhattacharyya D.; Metson J. & Evans P. (2005). Donor-acceptor pair luminescence of nitrogen-implanted ZnO single crystal, *J. Appl. Phys.* 97: 043528 (4 pages).

Yao B. D.; Chan Y. F. & Wang N. (2002). Formation of ZnO nanostructures by a simple way of thermal evaporation, *Appl. Phys. Lett.* 81: 757 (3 pages).

Yuan G. D.; Zhang W. J.; Jie J. S.; Fan X.; Zapien J. A.; Leung Y. H.; Luo L. B.; Wang P. F.; Lee C. S. & Lee S. T. (2008). p-type ZnO nanowire arrays, *Nano Lett.* 8(8): 2591-2597

Ye J. D.; Gu S. L.; Li F.; Zhu S. M.; Zhang R.; Shi Y.; Zheng Y. D.; Sun X. W.; Lo G. Q. & Kwong D. L. (2007). Correlation between carrier recombination and p-type doping in P monodoped and In–P codoped ZnO epilayers, *Appl. Phys. Lett.* 90: 152108

Zhang S. B., Wei S. H. & Zunger A. (2001), Intrinsic n-type versus p-type doping asymmetry and the defect physics of ZnO, *Phys. Rev. B.* 63: 075205 (7 pages)

Nanowires

Edited by Paola Prete

ISBN 978-953-7619-79-4

Hard cover, 414 pages

Publisher InTech

Published online 01, February, 2010

Published in print edition February, 2010

This volume is intended to orient the reader in the fast developing field of semiconductor nanowires, by providing a series of self-contained monographs focusing on various nanowire-related topics. Each monograph serves as a short review of previous results in the literature and description of methods used in the field, as well as a summary of the authors recent achievements on the subject. Each report provides a brief sketch of the historical background behind, the physical and/or chemical principles underlying a specific nanowire fabrication/characterization technique, or the experimental/theoretical methods used to study a given nanowire property or device. Despite the diverse topics covered, the volume does appear as a unit. The writing is generally clear and precise, and the numerous illustrations provide an easier understanding of the phenomena described. The volume contains 20 Chapters covering altogether many (although not all) semiconductors of technological interest, starting with the IV-IV group compounds (SiC and SiGe), carrying on with the binary and ternary compounds of the III-V (GaAs, AlGaAs, GaSb, InAs, GaP, InP, and GaN) and II-VI (HgTe, HgCdTe) families, the metal oxides (CuO, ZnO, ZnCoO, tungsten oxide, and PbTiO3), and finishing with Bi (a semimetal).

How to reference

In order to correctly reference this scholarly work, feel free to copy and paste the following:

B. Q. Cao, M. Lorenz, G. Zimmermann, C. Czekalla, M. Brandt, H. von Wenckstern, and M. Grundmann (2010). P-Type Phosphorus Doped ZnO Wires for Optoelectronic Applications, Nanowires, Paola Prete (Ed.), ISBN: 978-953-7619-79-4, InTech, Available from: http://www.intechopen.com/books/nanowires/p-type-phosphorus-doped-zno-wires-for-optoelectronic-applications

INTECH
open science | open minds